MDPI

Article

The feasibility of dynamic musculoskeletal function analysis of the vastus lateralis in endurance runners using continuous, hands-free ultrasound

Marloes Sjoerdsma [1,*], Cristina Caresio [1], Benjamin Tchang [1], Amber Meeder [1], Frans van de Vosse [1] and Richard Lopata [1]

[1] Photoacoustics & Ultrasound Laboratory Eindhoven (PULS/e), department of Biomedical Engineering, Eindhoven University of Technology, Groene Loper 5, 5612AE, Eindhoven, The Netherlands

* Correspondence: m.sjoerdsma@tue.nl; Tel.: +31 40 247 3047

Version February 5, 2021 submitted to Appl. Sci.

Abstract: Dynamic imaging of the skeletal muscles used to be strenuous and often impossible to perform manually. Accordingly, long-term dynamic musculoskeletal imaging has not been performed. The feasibility of long-term dynamic musculoskeletal functional analysis using hands-free ultrasound will be demonstrated in ten healthy endurance runners. After every kilometer, the *vastus lateralis* muscle was imaged whilst running using a fixated probe connected to a smart phone. The image quality was quantified by estimation of the probe-skin contact preservation and the field-of-view stability. Moreover, the pennation angles and muscle thicknesses were computed automatically. Long-term dynamic acquisition was successful in nine out of ten runners. Probe-skin contact loss ranged between 0 and 57 % of the gait cycle. The biggest change in field-of-view occurred during the first kilometer with an average decline in complex-wavelet structural similarity index of 0.21, followed by an onward total decrease of 0.09, on average. The mean pennation angle and thickness were approximately constant, with the average fluctuation being 0.94 degrees and 0.11 cm, respectively. The feasibility of long-term musculoskeletal function analysis has been demonstrated, with probe-skin contact loss the main limiting factor. Dynamic, hands-free ultrasound might enable research for a more profound insight in the prevention and rehabilitation of musculoskeletal injuries.

Keywords: musculoskeletal, dynamic ultrasound; vastus lateralis; hands-free ultrasound; marathon; endurance running; field-of-view stability; pennation angle; muscle thickness

1. Introduction

Musculoskeletal disorders affect 25% of the world population inducing prolonged inactivity and limiting daily activities, resulting in physical disabilities, poor quality of life, high economic costs, and a decreased labor capacity [1,2]. The pathophysiology of numerous musculoskeletal disorders is still poorly understood, and are hard to predict and prevent [3,4]. Moreover, understanding of musculoskeletal injury mechanisms and patterns may aid in diagnosis and injury prevention.

In athletes, risks of injury were observed to be associated with fatigue, weakness, previous injuries, and an imbalance between agonist and antagonist muscles [5]. Most injuries arise during movements across two joints [6]. Moreover, eccentric contractions are associated with a greater risk of injury [5,7]. Musculoskeletal disorders frequently lead to alterations in gait, resulting in secondary injuries. For the prevention of injuries becoming chronic, it is important to prevent repetition of trauma and to ensure full recovery prior to maximal loading of the previously injured muscle [5]. In some cases, symptoms only show during exercise, due to motion related

changes (e.g. muscle/tissue swelling, fatigue, friction, impact forces). Dynamic assessment of muscle architectural and mechanical parameters might attribute in the diagnosis of muscle-related impairments. Additionally, dynamic evaluation might provide more information on the origin and possible prevention of the musculoskeletal disorders caused by exercise, atrophy, disease, and ageing [8].

In the clinic, physical examination is used for muscle and joint function quantification (e.g. strength, range of motion) [9–11]. Electrical activation of the muscles is investigated using electromyography [12–14]. Joint kinetics and kinematics can be measured using 3-D motion capture systems and ground force plates [15–17]. However, to obtain a more profound and realistic understanding of muscle function in dynamic conditions, imaging of the muscle whilst performing exercise would be promising.

Ultrasound is generally the most suitable imaging modality in the musculoskeletal system. The benefits of ultrasound include a high spatial and temporal resolution, useful for detection of anatomical structures and motion analysis, respectively. Moreover, ultrasound is economical, cheap, non-invasive, safe for both the examiner and the subject, portable, and has a relatively short acquisition procedure. In musculoskeletal ultrasound, the muscle architecture can be shown including the aponeuroses, and muscle fascicles. The architectural muscle parameters that can be analyzed using ultrasound contain pennation angles, fascia lengths, and muscle thickness [18–20]. Dynamically assessed parameters include contraction velocity, strain, stiffness during muscle contractions, and fascia length in relation to exerted force [4,21]. Furthermore, the echo intensity of the muscle area might expose neurological disorders or is an indication of muscle acidification [22]. Structures adhering to the muscle (e.g. tendons and its fibers, cartilage, bursa, bones) can also be visualized with high quality [23,24].

Dynamic imaging of the skeletal muscles is strenuous and often impossible to perform manually, since the transducer has to be held in a fixed position. Manual acquisitions might be feasible during low intensity exercise, though the musculoskeletal function parameters are likely to vary between different exercise intensity levels. In static interval measurements, the imaging plane is difficult to reproduce. Out-of-plane motion as a consequence of an unstable field-of-view renders measurements such as Doppler velocity imaging and strain impossible. A constant field-of-view is crucial for accurate estimation of muscle tissue parameters [25].

Fixation of the transducer enables dynamic imaging, and has been shown to overcome part of the limitations associated with manual acquisitions. Probe fixation has been shown to yield improved or similar field-of-view stability and repeatability of ultrasound acquisitions [18,26,27]. Additionally, probe fixation has shown to decline shoulder abduction and forearm muscle activation of sonographers without influencing the acquisition time in echocardiography [28]. A demonstration of short-term probe fixation during a few minutes of cycling exercise was already presented [18]. However, the feasibility of dynamic musculoskeletal ultrasound acquisitions during long-term (running) exercise still has to be demonstrated.

In this study, the feasibility of obtaining dynamic ultrasound acquisitions and evaluating the skeletal muscle function is investigated in ten endurance runners. To the best of our knowledge, no hands-free, outdoor, long distance, ultrasound acquisitions have been obtained previously. In endurance running, the risk of probe displacement due to external factors (e.g. other participants, attributes, the ground) is minimal. Additionally, in endurance running, the exercise performed is fairly invariable, implying deviations in functional measurements are most likely caused by probe dislocation or detachment [29,30].

The objectives of this study were to quantitatively analyze the image quality and demonstrate the possibility of functional parameter computation from ultrasound images obtained hands-free during endurance exercise. The image quality was assessed by estimation of maintained probe-skin contact,

and field-of-view stability analysis using the complex-wavelet structural similarity index method (CW-SSIM). Potential probe-skin contact loss was expected to occur due to sweating, or slight probe fixation device shifts. The field-of-view was hypothesized to stay constant, based on a previous study executed during a couple of minutes of cycling exercise [18]. Furthermore, the functional measurements were expected to remain constant over time and distance ran, since this study was performed during endurance exercise. The pennation angle and muscle thickness have shown to remain constant when measured prior and post endurance running [29–31].

2. Materials and Methods

Participants

Nine healthy trained endurance runners were asked to participate in this study, of which two subject participated twice. The volunteers consisted of five males and four females between the age of 25 and 35 with no musculoskeletal injuries or known cardiovascular abnormalities. Unfortunately, one of the female runners was excluded from the study, since the fixated probe lost contact after running three kilometers. All runners were already enrolled in a professionally organized endurance running event prior to recruitment.

The local Medical Ethics Committee of the Máxima Medical Centre, Veldhoven, The Netherlands waived ethical approval (N18.124, October 12, 2018, and N19.076, September 16, 2019). In 2017, the study involved measurements with CE marked devices on endurance runners, who were not specifically asked to participate in a professionally organized endurance running event for this study, and all gave their written informed consent for the ultrasound measurements during the endurance running event. For that purpose, protocol evaluation by a METC was not considered standard practice at the time, which encompasses three volunteers. All volunteers provided written consent. The procedures were carried out in accordance with the Declaration of Helsinki.

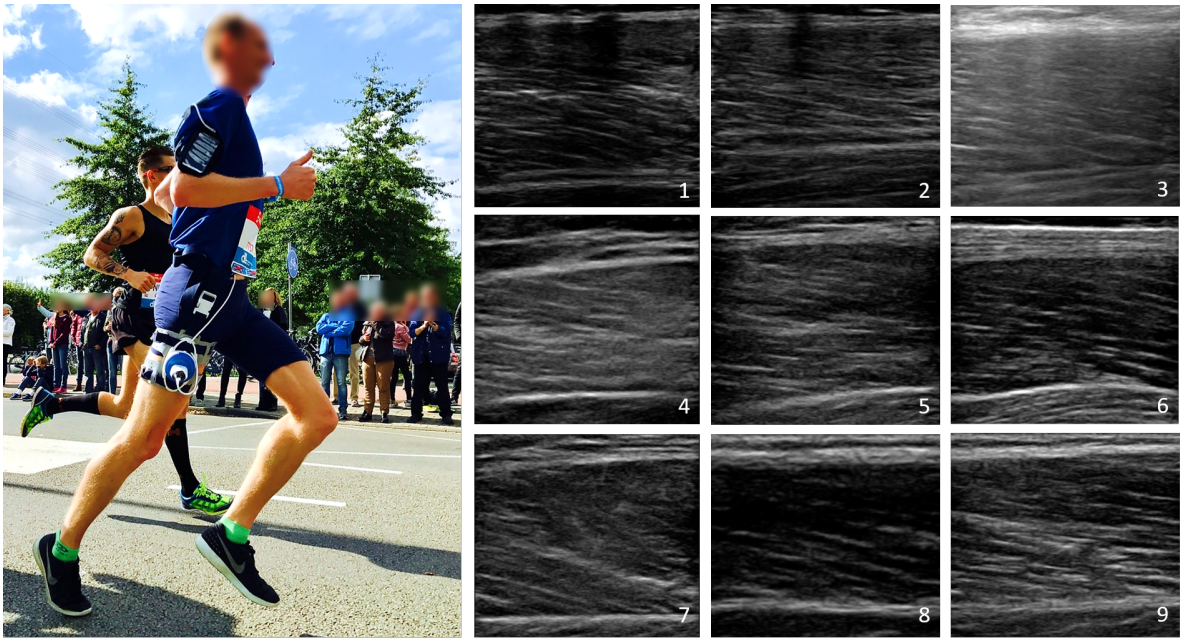

Figure 1. *Experimental set-up of the endurance runners. (Left) The transducer is fixated onto the upper leg to image the belly of the vastus lateralis muscle in the longitudinal direction. The transducer is connected to a mobile phone, which is attached to the upper arm of the volunteer. (Right) A representative ultrasound image obtained at the 5th kilometer of all included volunteers.*

Acquisition protocols and equipment

A portable, broadband linear array transducer (Lumify L12-4, Philips, USA) with ultrasonic gel (Aquasonic 100 Ultrasonic Gel, Parker) was embedded in a fixation device (ProbeFix Dynamic, USONO, Eindhoven, The Netherlands), which was attached to the right leg of the participant. The imaging plane encompassed the belly of the vastus lateralis muscle in the longitudinal cross section. The transducer was connected to a smartphone, which was attached to the right upper arm of the participants. Nine of the participants engaged in half a Marathon (21 km) and one participant ran 10 km during another professionally organized event.

After approximately every kilometer, the participants acquired ten seconds of conventional 2-D ultrasound images using the Lumify ultrasound application on their smart phone, whilst running. These interval acquisitions were repeated until complete battery depletion occurred, or the finish line was reached. Acquisitions were started after the first kilometer to account for possible probe shifts whilst initiating exercise. The B-mode ultrasound images were acquired at a frame rate of 24 to 30 Hz and with imaging depths between 3.5 and 6.0 cm. The musculoskeletal, vascular, and lung presets were used in volunteers 1 and 2, 3, and 4 - 10, respectively. The different presets were employed to determine the optimal image setting for dynamic acquisitions. In the volunteers, the imaging parameters were kept constant as long as probe-skin contact was still preserved during part of the gait cycle.

Data analysis

The ultrasound data were transferred to an external computer in DICOM format. These DICOM files were analyzed by algorithms implemented in MATLAB (MATLAB 2018b, MathWorks, Natick, MA, USA).

Image decomposition

For the structural similarity analysis, and the detection of aponeuroses and muscle fascicles, the ultrasound images were decomposed using a steerable, oriented pyramid employing complex and oriented wavelets [32]. The oriented wavelets were created by successive application of low and high pass filters, and a mask selecting only a specific orientation range of the resulting bandpass filter. Additionally, complex instead of real wavelets were employed, since most structure information is provided by the relative phase patterns of the wavelet coefficients [33].
In this study, the frequency spectra of the ultrasound images were separated using maximally six decomposition levels. The detail images resulting from this decomposition contained image structures of an increasing size range with increasing decomposition level (Table 1). Orientation zero of the wavelets was defined as 0 rad, which was parallel to the ultrasound beam, and was incrementally increased with $\frac{\pi}{n}$ rad, with n the number of chosen orientations.

Table 1. *Full width at half maximum ranges of the bandpass filters in the spatial domain. The pixel sizes of the acquisitions ranged between 0.07 and 0.15 mm*

Decomposition level	Bandpass filter size range (pixels)
1	1.5 - 2.6
2	3.0 - 5.3
3	5.8 - 10.4
4	11.4 - 20.2
5	21.6 - 38.9
6	41.7 - 73.0

Image quality

Image quality quantification was performed through probe-skin contact preservation assessment, and field-of-view stability evaluation measured using the complex-wave structural similarity index.

Probe-skin contact

Probe-skin contact loss might occur due to sweating, the cyclic motion of the legs, and the impact forces from the ground. Accordingly, the duration percentage of probe-skin contact was quantified for all acquisitions. In case the transducer lost complete contact with the skin, a black ultrasound image was observed with a bright, white, hyper-echoic line-shaped artifact present near the transducer position, resulting from the high acoustic impedance between the ultrasound transducer and air causing total reflection (Fig. 3a). Hence, contact loss was empirically defined as a frame containing a black area of at least 80 % of the image.

Field-of-view stability

The field-of-view stability was evaluated utilizing the complex wavelet structural similarity index method (CW-SSIM). The CW-SSIM is a full-reference method based on human vision, which compares the structures visible within an image to those of a chosen reference image. The similarity between the images is computed using the brightness (mean pixel intensity), contrast (variance), and image structures (covariance) [34]. The CW-SSIM has been shown to be an adequate comparison method for ultrasound data [35], since it compares the detail images of the highest decomposition level. Accordingly, the method a) disregards noise and ultrasound speckle, b) predominantly compares the principal image features, and c) adopts the benefit of the relatively higher precision with which lower frequencies can be determined. Moreover, small rigid rotations and translations, and modest image brightness alterations have no effect on the CW-SSIM index. For example, a brightness modification of 10% leads to a CW-SSIM index reduction from its maximum value 1 to minimally 0.996 [34]. The CW-SSIM index will decrease to approximately zero in case the image structures are completely different, and will be equal to one in case the images compared are identical.

Prior to the CW-SSIM analysis, the images were decomposed as previously described, using six levels and 16 orientations. For each of the 16 oriented detail images of level six, the local CW-SSIM indices are computed using:

$$S(c_I, c_{II}) = \frac{2|\sum c_{I,i}\, c^*_{II,i}|}{\sum |c_{I,i}|^2 + \sum |c_{II,i}|^2} \quad (1)$$

with $c_I = \{c_{I,i} | i = 1, ..., N\}$ and $c_{II} = \{c_{II,i} | i = 1, ..., N\}$ the local wavelet coefficients acquired from the same spatial location in the oriented detail image of the reference image and the image it is being compared to, and c^* the complex conjugate of c [34]. These local CW-SSIM indices are combined into a single index per oriented detail image using a 7 x 7 Gaussian filter. The standard deviation of the Gaussian was defined as a quarter of the size of the detail image [34]. Subsequently, the mean of the CW-SSIM indices of the oriented detail images is obtained, resulting in the final CW-SSIM index describing the similarity between the two images.

In this study, the CW-SSIM indices over time were obtained by calculating a representative CW-SSIM index. The representative CW-SSIM indices were calculated from the ten second ultrasound clips, which were obtained after every kilometer ran by the athlete. Ten randomly chosen reference frames of first and the previous acquisition were compared to all frames of an ultrasound clip. The random choice of reference frames prevented bias and ensured the inclusion of reference frames from different time points in the gait cycle. For every reference frame, the ten highest CW-SSIM indices were considered, since every acquisition contained minimally ten gait cycles, and averaged. Finally,

for every kilometer, the maximum of the ten averaged CW-SSIM indices was taken, to obtain the representative CW-SSIM index. Frames showing probe-skin contact loss were excluded from the field-of-view stability analysis.

Functional evaluation

For functional evaluation, the muscle thickness and pennation angle of the fascicles were computed. For this computation, an adapted version of the method described in Heres et al. [18] was used, which was optimized for the imaging settings used in this study.
First of all, the frequency spectra of the images were decomposed, as explained previously, into five levels with four orientations. Each level of detail images contains a specific structure size range (Table 1). Accordingly, for aponeurosis detection level 5 was used, whereas for fascicle detection levels 2-4 were adopted (Fig. 2, 2nd step). For both, the third orientation (π rad) was used, since the structures selected from this orientation are perpendicular to the ultrasound beam. Selection of only this orientation leads to a reduction in noise in the resulting detail images depicting the aponeuroses and fascicles. Subsequently, an adaptive threshold was applied to the detail images of the aponeuroses and fascicles [36], which segmented the image into three clusters with minimal variance within each cluster. Finally, the clusters containing the aponeuroses or fascicles was selected (Fig. 2, 3rd step).

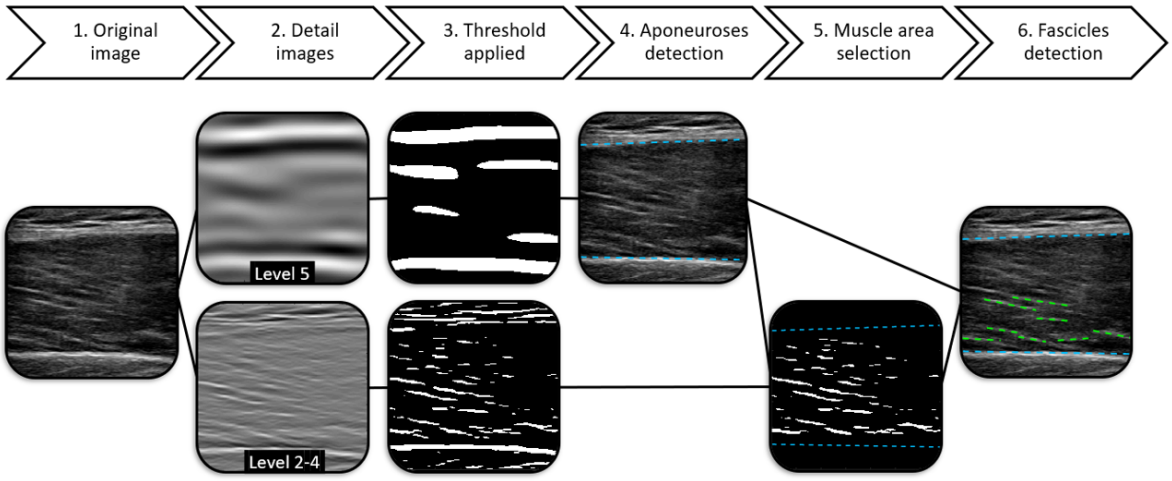

Figure 2. *The workflow of the muscle architecture detection. (1) The original image (2) is decomposed into five oriented detail images with four orientations. Level 2-4 and level 5 are used for fascicles and aponeuroses detection, respectively. For both, the structure orientation perpendicular to the ultrasound beam is used. (3) Subsequently, a threshold is applied to the detail images of the aponeuroses and fascicles. (4) In the aponeuroses detail image, the edges of the anterior and posterior aponeurosis adhering to the muscle are identified, respectively. (5) Only the region between these aponeuroses is selected for fascicles detection. (6) The detected aponeuroses and fascicles super imposed onto the original image.*

For aponeurosis detection, the coordinates of the middle point of the anterior and posterior aponeurosis were manually selected in the first frame only. In some cases, another collagen structure was present near the aponeuroses. Therefore, for both the anterior and posterior aponeurosis, the biggest structure was selected in the detail image depicting the aponeuroses within a range of $\pm$ two millimeters from these manually selected coordinates. The coordinates of the two points were updated to the center of the selected biggest structures within this four millimeter range. Subsequently, the edges of the anterior and posterior aponeurosis adhering to the muscle were detected. A first order polynomial was fit through these edges, resulting in the segmentation of the muscle (Fig. 2, 4th step).

The anterior-posterior muscle thickness was estimated by averaging the vertical distances between both segmented edges for the entire field-of-view. In rare cases, a thick muscle fiber bundle was captured as the posterior aponeurosis. Hence, in case the angle of the posterior aponeurosis was bigger than three degrees, the frame was ignored in the functional analysis. In some frames, an artery was visible and mistaken for aponeurosis. These falsely detected aponeuroses were excluded through visual inspection.

For fascicle detection, the segmented muscle area was selected in the thresholded detail image displaying the fascicles (Fig. 2, 5^{th} step). The outer two millimeters of the selected area were disregarded, since these regions mostly contained noisy structures, which affected fascicles detection negatively. In addition, all structures smaller than the empirically determined threshold of 200 pixels were also removed, since these were too small for pennation angle computation. Through the remainder of the structures within the muscle, a first polynomial was fit through the center of masses of the left and right part of each fascicle (Fig. 2, last step). Subsequently, the pennation angle of the fascicles was calculated with respect to the posterior aponeurosis. A representative pennation angle per frame was estimated by obtaining the median of the pennation angles within the frame.

3. Results

The datasets from nine out of the ten volunteers were analyzed during post-processing, since in one of the volunteers the probe and its fixation device lost complete contact after running three kilometers. Only in one of the subjects, acquisitions were obtained during the full race. In the other subjects, the battery died prior to finishing the race. In subjects 8 and 9, the straps of the fixation device were tightened after running 11 kilometers. In the remainder of the subjects, the probe and its fixation stayed in the same position, without manual interference during the measurements. The best image quality for the dynamic musculoskeletal measurements was produced using the ultrasound preset named "Lung" (Fig. 1: 4 - 9). In this preset, image contrast was highest and the persistence (i.e. temporal compounding) seemed minimized. In the musculoskeletal preset, persistence was high, resulting in the visualization of artificial aponeuroses and fascicles, due to averaging of previous frames (Fig. 1: 1 & 2). In the vascular preset, the persistence was high, the contrast was relatively low, and the proximal aponeurosis was hyper-echoic, hampering functional analysis (Fig. 1: 3).

Image quality

The image quality was quantified by estimation of the probe-skin contact preservation and field-of-view stability.

Probe-skin contact was preserved for the full duration of the measurements in four volunteers. In the other five included volunteers, some probe-skin contact loss was observed, which occurred cyclically during part of the gait cycle (Fig. 3b). The degree of this contact loss ranged from 6 - 57 % of the gait cycle (Fig. 3c).

The field-of-view stability was measured using the CW-SSIM. For each acquisition, a representative CW-SSIM index was computed (Fig. 4). The CW-SSIM indices with respect to the first acquisition reduced slightly over time (Fig. 4a). The difference in CW-SSIM index between the last and second acquisition was 0.09 ± 0.06 . The average difference between the first and second acquisition was largest, being 0.21 ± 0.12. In runners 1 and 2, the CW-SSIM indices were relatively lower, which were acquired using the musculoskeletal preset.

The CW-SSIM indices with respect to the previous acquisitions were roughly constant. The average similarity with respect to the previous acquisition was quantified using a CW-SSIM index of 0.85 ± 0.08. Again, the structural similarities of the first two volunteers were smaller due to the use of a less optimal preset.

For most acquisitions, a portion of the acquisitions was adequate for functional analysis (46

± 27 % of the full acquisition). Only in 13% of the acquisitions the image quality was sufficient to perform functional computations throughout almost the full acquisition. In most acquisitions, parts of the acquisition could not be analyzed due to inadequate image quality caused by either probe-skin contact loss (6 - 57 % of each gait cycle, see Figure 3), the presence of an artery in the imaging plane close to the posterior aponeurosis (only occurred in volunteer 1 in two acquisitions), detection of an artificial posterior aponeurosis resulting from temporal compounding (main issue in subjects 1-3), or hypo-echoicity of the posterior aponeurosis (only 1-3 frames of most gait cycles). The probe-skin contact loss, hypo-echoicity of the aponeurosis, or especially the combination of probe-skin contact loss and hypo-echoicity of the aponeurosis resulted frequently in the inability to detect the aponeuroses in the next few frames, or a full or multiple gait cycles in a row.

Functional evaluation

A demonstration of functional measurements during endurance running is shown by measuring the thickness of the *vastus lateralis* muscle and its pennation angles. These dynamic functional measurements were performed for each ultrasound recording of ten seconds obtained successively after running a kilometer. Subfigures 5a and b depict an example of these dynamic functional measurements. In these subfigures, the muscle thickness is displayed using repeating segments, with each individual segment representing a single gait cycle. The pennation angle also shows variation within the 10 second interval, though the individual gait cycles are less clearly distinguishable.
For each kilometer, the mean thickness and pennation angle were calculated, which are illustrated in Subfigures 5c and d. The mean muscle thickness ranged between 1.29 and 2.50 cm, and the mean pennation angles ranged between 1.3 and 12.8 degrees.
The error bars in these subfigures 5c and d are the standard deviations representing parameter variation related to the gait cycle. Hence, the bars give an impression of the muscle's contraction force of each gait cycle independently. Both the mean values and their standard deviations of these functional parameters remained approximately constant. The average fluctuation of the muscle thickness and the pennation angles over time were 0.11 cm and 0.94 degrees, respectively. The mean standard deviation of the error bars of the thickness and pennation angle were 0.038 cm and 0.41 degrees, respectively.

4. Discussion

The introduction of portable ultrasound systems and ultrasound transducer fixation devices has made dynamic evaluation of the skeletal muscles possible. The feasibility of short-term dynamic ultrasound acquisitions has already been demonstrated previously in cycling exercise in ultrasonography of skeletal muscles and in echocardiography [18,27]. In this study, the feasibility of long-term dynamic functional measurements has been investigated in ten endurance runners. Endurance runners were selected as participants for this research, since their labor is relatively invariable and there is no danger of fixated transducer motion as a consequence of external forces (e.g. contact with other athletes, attributes, or the ground). In addition, the forces that are generated when the feet come into contact with the ground might also have an effect on the feasibility of long-term dynamic acquisitions during endurance running.

When using an ultrasound transducer designed for smart mobile usage, usually only the preset, gain, and power can be modified. In this study, a linear array Philips Lumify L12-4 was used. For this transducer, five presets were available (i.e. lung, musculoskeletal, soft tissue, superficial, and vascular), each optimized for their specific application. The musculoskeletal preset was most likely optimized for static acquisitions, since it has a high persistence (i.e. temporal compounding). A high persistence in static musculoskeletal acquisitions will lead to an augmented contrast and a reduction in noise. However, in dynamic measurements high persistence results in the materialization of artificial

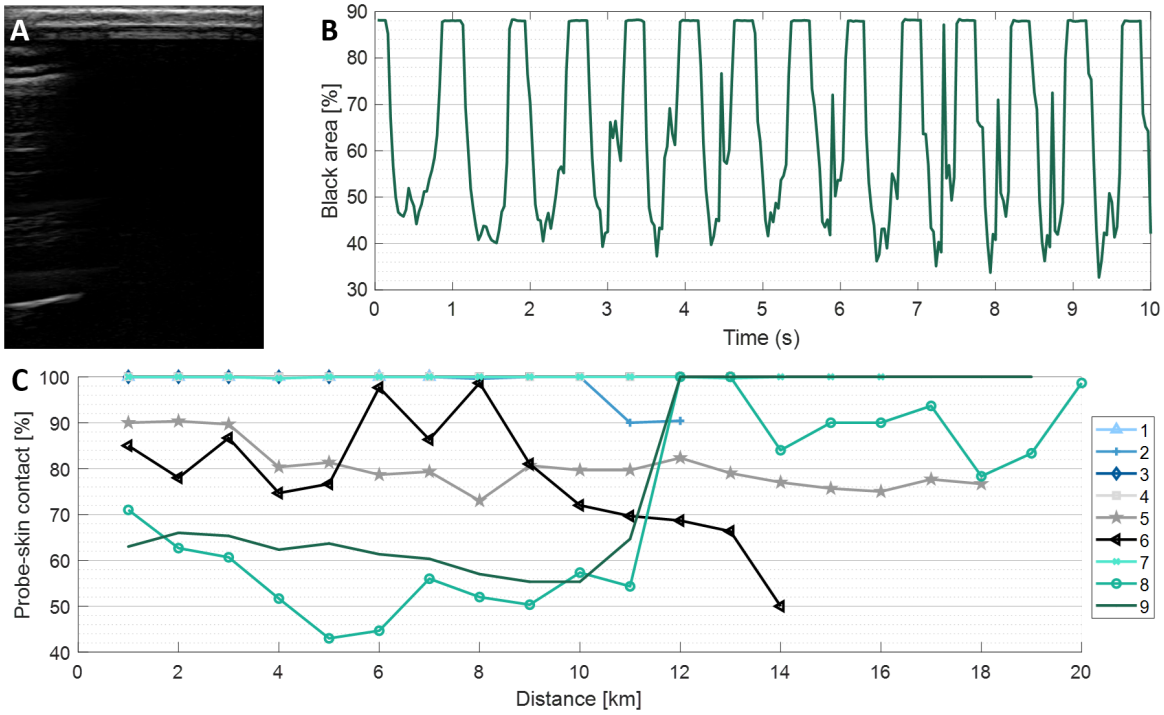

Figure 3. *Probe-skin contact. (a) An example of an ultrasound image obtained during probe-skin contact loss. The right part of the frame shows a total reflection artifact, caused by a big difference in acoustic impedance between the ultrasound probe and the air. At the left side some probe-skin contact is still preserved. (b) A representative example of an acquisition during which probe-skin contact loss occurred. Probe-skin contact was defined as an ultrasound frame consisting of less than 80% black pixels. This example was acquired during the first kilometer of volunteer 9. As shown in the subfigure, contact loss occurs cyclically during the same phase of the gait cycle, which was the case in all volunteers with probe-skin contact loss. (c) The percentage of frames within the acquisition that was obtained with preserved probe-skin contact. In four subject, probe-skin contact was preserved during the entire measurement. In the other five volunteers, the probe was in contact with the skin during 43 - 100 % of the gait cycle.*

posterior aponeuroses. Therefore, the musculoskeletal preset is deficient for dynamic measurements. In the vascular preset, the persistence appeared to be higher and the contrast lower in comparison to the musculoskeletal preset. Consequently, the aponeuroses detection algorithm failed to track the posterior aponeurosis during the gait cycle. Hence, this dataset was excluded from functional evaluation. The lung preset was most suitable for these dynamic measurements, since the contrast was sufficient and no temporal compounding seemed to be applied.

The image quality was evaluated by quantification of probe-skin contact preservation and the field-of-view stability. In four volunteers, the probe-skin contact was preserved during the entire measurement. However, in five volunteers, temporary probe-skin contact loss occurred for some or all acquisitions. Probe-skin contact loss could be a result of gel loss caused by sweating, a slight probe displacement, muscle deformation during contraction, or by probe dislocation induced by gravitational pull or inertia of the probe motion countered by the ground impact forces. Within an acquisition, probe-skin contact loss occurred during part of the gait, which was approximately identical for each gait cycle captured within the acquisition. Although functional analysis of the complete gait cycle was impossible in these acquisitions, functional parameter alterations within these gait sections over time still contain valuable information.

The field-of-view stability was estimated using the CW-SSIM. The initial CW-SSIM index drop was highest, which could be caused by a dislocation of the transducer, or by a general temporal

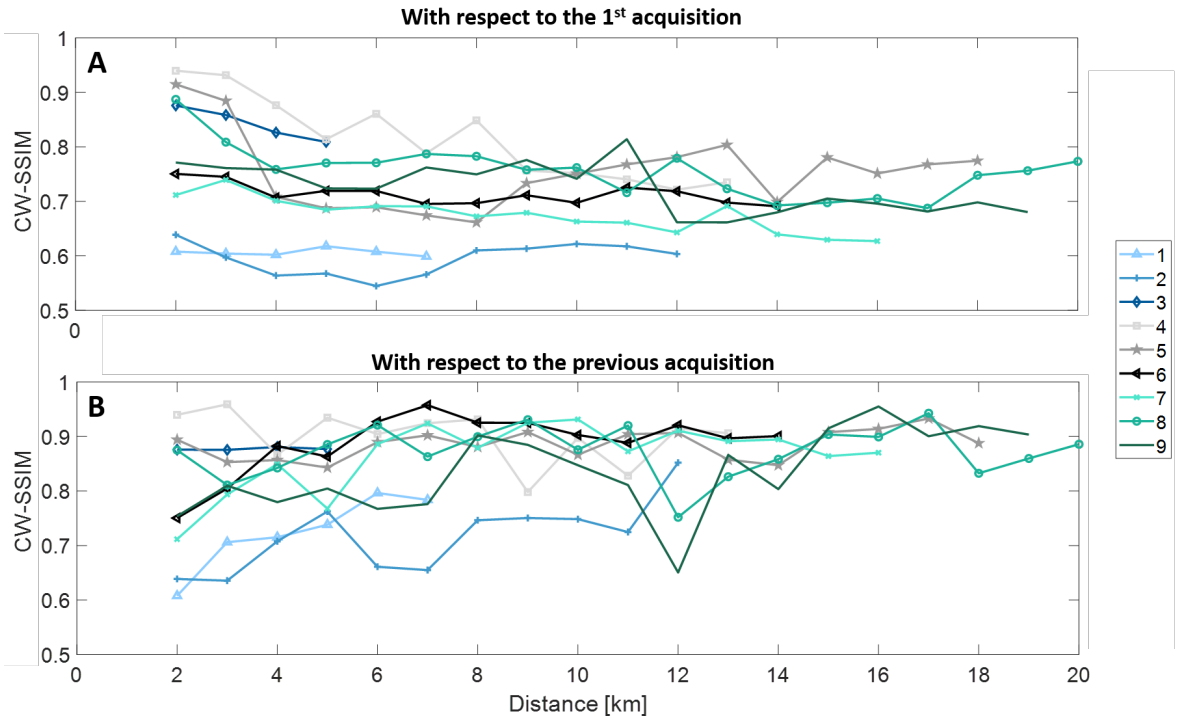

Figure 4. *Field-of-view stability. (a) The complex-wavelet structural similarity index method values of each acquisition with respect to the first acquisition obtained after the first kilometer. The difference between CW-SSIM indices between the last and second acquisition is on average 0.09. (b) The CW-SSIM indices with respect to the previous acquisition, which was on average 0.85. The CW-SSIM indices of volunteer 1 and 2 are relatively lower, which were acquired using a different preset.*

decorrelation of the ultrasound images provoked by noise and/or slight out-of-imaging-plane motion. A dislocation of the transducer would result in a relatively big alteration in the measured functional parameters. However, the difference in muscle thickness and pennation angle between the first and second kilometer is comparable to the average variation of these functional parameters. Accordingly, the initial drop in CW-SSIM indices is expected to be caused by temporal decorrelation.

The functional parameters in this study consisted of the muscle thickness and pennation angles of the fascia with respect to the posterior aponeurosis. In eight out of nine runners, a sufficient portion of gait cycle could be analyzed. The excluded dataset was acquired using the vascular preset resulting in poor image contrast, and the display of extra artificial posterior aponeuroses, as explained previously. The average values of the functional parameters remained fairly constant throughout the race, which is expected based on literature studies examining alterations in muscle thickness and pennation angles in endurance runners and resistance training [29–31]. In these studies, the muscle thickness and pennation angles are measured statically prior and post training. These studies showed no adaptions in muscle thickness and pennation angle after 10 weeks of endurance running or after running a marathon, whereas during resistance training augmentations of both parameters were observed. However, it should be noted that in this study the ultrasound measurements were performed dynamically instead of the static ultrasound measurements performed in the previously mentioned studies. Still, the stability of both functional parameters suggests the preservation of field-of-view throughout the race.

The functional parameter fluctuations observed throughout the gait cycles are a consequence of muscle contraction. Moreover, during contraction, out-of-plane motion occurred to some degree in all runners. The muscle contraction-related variations are similar in all endurance runners and remained roughly constant over time.

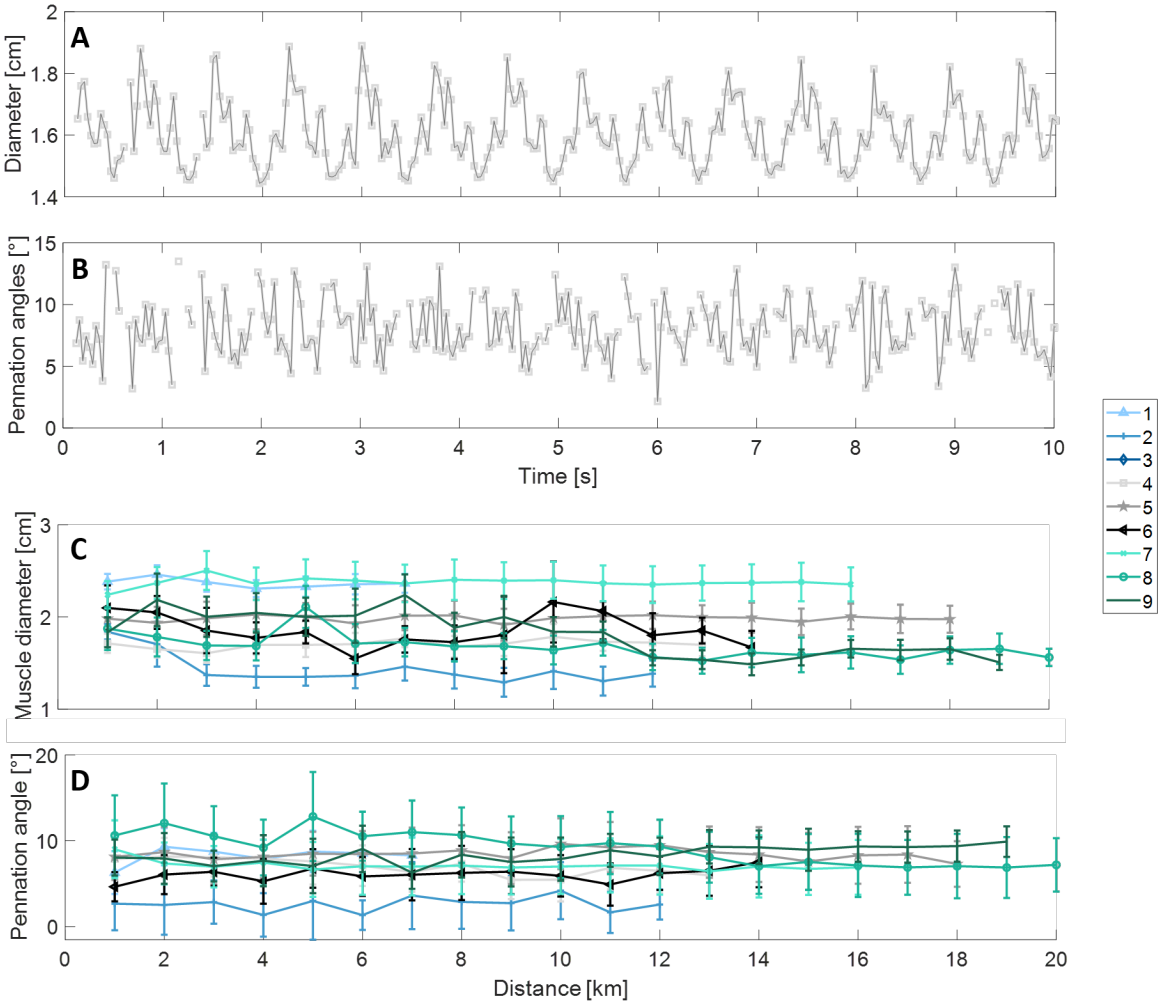

Figure 5. *Dynamic functional measurements. For all acquisitions, the thickness of the muscle and the pennation angle of the fascicles are computed. (a) and (b) are examples of these computations. These two examples were derived from the ultrasound images obtained at the 7th kilometer in subject 4. In (a) the cyclic contraction of the muscle is visible, whereas the pennation angles contain relatively more noise. (c) and (d) display the mean muscle thickness and the pennation angle for all kilometers. The error bars show the standard deviation of each acquisition, representing the variation within the gait cycle, which is a result from muscle contraction. The muscle thickness and pennation angle are roughly contact over time.*

The feasibility of long-term dynamic ultrasound image acquisition and functional evaluation of the *vastus lateralis* has been demonstrated. However, some limitations were observed in this study. The main limiting factor was the inability to acquire functional and architectural information throughout the complete gait cycle in most subjects, which was mainly caused by probe-skin contact loss. However, probe-skin contact loss could be overcome by the incorporation of a dedicated gel patch during the acquisitions or by further optimization of the probe fixation device. The frequency and the impact of the issues hampering posterior aponeurosis detection (e.g. hypo-echoicity of aponeurosis) are expected to decrease largely once the probe-skin contact loss has been minimized. Additionally, the currently used algorithm could be improved further by taking into account an estimation of the aponeurosis motion during a gait cycle based on the successfully analyzed frames of (other) gait cycles. Alternatively, deep learning models could be used for feature detection [8,37].

3-D acquisitions could further improve the dynamic functional evaluation. In 3-D ultrasound, out-of-plane motions can be tracked and stabilized during post-processing. Furthermore, feature

detection and functional assessment of architectural and mechanical parameters is expected be more robust. Therefore, local functional analysis will also be improved in 3-D. However, the effect of the spatial and temporal resolution reduction on the performance of the dynamic functional measurements should be analyzed. Moreover, there are no 3-D portable US systems on the market, which is due to the higher level of complexity in both hard- and software. Additionally, the use of ultrafast imaging would be beneficial for the analyses proposed, but an ultrafast portable solution is also unavailable.

The results observed in this study are expected to be applicable to other muscles situated in the leg or arm. Hands-free, continuous ultrasound acquisitions are applicable in the field of sports to analyze and improve muscle activation and motion, and gait. Monitoring of the muscles during exercise could also aid in the creation of optimized training schemes, or in the assessment of the athlete's fitness level.
Another application of hands-free, continuous ultrasound evaluation of the muscle is during the revalidation process after a muscle injury. The acquisitions could help to determine when it is safe to return to play with minimal chance of injury repetition.
In other ultrasound fields, the application of hands-free, continuous acquisitions could also be beneficial. In echocardiography, upright, continuous, hands-free stress echocardiography could be performed, leading to a reduction in image plane variation between exercise levels. Additionally, this method could be applied for continuous cardiac monitoring in the intensive care, or during operations, since transthoracic echocardiography has shown to be able to detect ischemic events that are difficult to recognize using ECG or other widely used hemodynamic monitoring parameters [38].
Furthermore, the use of a fixation device could reduce the prevalence of work-related musculoskeletal disorders amidst sonographers. The high quantity of ultrasound exams performed resulted in repetitive strain injury symptoms to be experienced by ninety percent of the sonographers despite corrections in their posture and the use of an adjustable working space [39,40]. In echocardiography, probe fixation has shown to reduce muscle contraction in the forearm and total shoulder abduction time, without extending the exam duration [28].

In future studies, a larger group of endurance runners should be included. Once the current limitations are overcome, functional parameters can be measured during the full gait cycle. These continuous functional measurements may aid in the detection of gait cycle modifications resulting from fatigue. Alternatively, differences in gait between trained and untrained runners, or during different stages of the revalidation process might be detected. These differences in gait might be used for gait correction, which may aid in the prevention of injury or avoid injury repetition. In addition, the combined acquisition of ultrasound and electromyography, could lead to additional relevant dynamic information of muscle activation during exercise.
This study encourages the dynamic computation of local functional parameters (e.g. individual pennation angles, fascia lengths, local strain and strain rates). Global functional assessment is limited by the independency between muscle architecture and activity. Additionally, various disorders manifest themselves locally [4,41]. Furthermore, muscles contain different fiber types of which the response varies with exercise intensity and duration [41]. Local parameters might provide a more profound insight in musculoskeletal disorders and facilitate monitoring of training progression in athletes.
Future research using dynamic, hands-free ultrasound might provide identification markers for fatigue (e.g. pennation angle increase, reduction in motor unit recruitment, local alterations in muscle stiffness), which can contribute to injury or musculoskeletal disorder prevention, and may help drafting optimal practice schemes for professional athletes. Furthermore, local, dynamic monitoring of muscle architecture and characteristics might provide an indication when a patient or injured athlete is able to perform exercise again with a low risk of re-injury, or the injury becoming chronic [42]. It is unclear which rehabilitation program is most successful for different types of injuries and how

much effect the local muscle characteristics have on injury risks. Therefore, further research on these parameters in the rehabilitation using dynamic ultrasound could be valuable.

5. Conclusions

The feasibility of functional measurements in the *vastus lateralis* muscle has been demonstrated during endurance running. After running the first kilometer, the field-of-view stability remained high during the remainder of the race. Although probe-skin contact loss was the study's main limiting factor, a section or the complete gait cycle could be visualized and analyzed in all endurance runners in all obtained ultrasound acquisitions. Computation of the pennation angle and muscle thickness were successful in part of or almost the full gait cycle. These functional parameters remained approximately stable throughout the measurement. These findings are expected to be extendable to the application on other muscles.

Author Contributions: Conceptualization: M.S., C.C., A.M., B.T., F.V. and R.L.; methodology: M.S., C.C., A.M., B.T. and R.L.; software: M.S.; validation: M.S.; formal analysis: M.S.; investigation: B.T., C.C. and A.M. ; resources: B.T., A.M., F.V. and R.L.; data curation: M.S., C.C., B.T. and A.M.; writing–original draft preparation: M.S.; writing–review and editing: M.S., C.C., A.M., B.T., F.V. and R.L.; visualization: M.S.; supervision: C.C. and R.L.; project administration: F.V. and R.L.; funding acquisition: R.L. All authors have read and agreed to the published version of the manuscript.

Institutional Review Board Statement: The study was conducted according to the guidelines of the Declaration of Helsinki. Ethical review and approval were waived by the local Medical Ethics Committee of the Máxima Medical Centre, Veldhoven, The Netherlands, since the research conducted does not fall under the scope of the Medical Research Involving Human Subjects Act (N18.124, October 12, 2018, and N19.076, September 16, 2019). In 2017, the study involved measurements with CE marked devices on endurance runners, who were not specifically recruited and asked to participate in a professionally organized endurance running event for this study. These three runners gave their written informed consent for the ultrasound measurements during the endurance running event. For this purpose, protocol validation by a METC Committee was not best practice at the time. For all volunteers written informed consent was obtained.

Informed Consent Statement: Informed consent was obtained from all subjects involved in the study.

Funding: This work is part of the MUSE project, which has received funding from the European Research Council (ERC) under the European Union's Horizon 2020 research and innovation programme (ERC starting grant 757958).

Conflicts of Interest: The authors declare no conflict of interest, except for B.T. who also worked at USONO at the time of experiment conduction. The funders had no role in the design of the study; in the collection, analyses, or interpretation of data; in the writing of the manuscript, or in the decision to publish the results.

Abbreviations

The following abbreviation is used in this manuscript:

CW-SSIM	complex-wavelet structural similarity index method

References

1. for Health Statistics (US), N.C. *National Health Interview Survey: research for the 1995-2004 redesign*; Number 121-126, US Government Printing Office, 1999.
2. Reginster, J.Y. The prevalence and burden of arthritis. *Rheumatology* **2002**, *41*, 3–6.
3. Swentik, A. Pathophysiology of Skeletal Muscle Injury. In *Muscular Injuries in the Posterior Leg*; Springer, 2016; pp. 35–47.
4. Eranki, A.; Cortes, N.; Ferenček, Z.G.; Sikdar, S. A novel application of musculoskeletal ultrasound imaging. *JoVE (Journal of Visualized Experiments)* **2013**, p. e50595.
5. Whiting, W.C.; Zernicke, R.F. *Biomechanics of musculoskeletal injury*; Human Kinetics, 2008.

6. Page, P. Pathophysiology of acute exercise-induced muscular injury: clinical implications. *Journal of athletic training* **1995**, *30*, 29.
7. Järvinen, T.A.; Järvinen, T.L.; Kääriäinen, M.; Kalimo, H.; Järvinen, M. Muscle injuries: biology and treatment. *The American journal of sports medicine* **2005**, *33*, 745–764.
8. Cunningham, R.; Sánchez, M.B.; May, G.; Loram, I. Estimating full regional skeletal muscle fibre orientation from B-mode ultrasound images using convolutional, residual, and deconvolutional neural networks. *Journal of Imaging* **2018**, *4*, 29.
9. Beaudart, C.; Rolland, Y.; Cruz-Jentoft, A.J.; Bauer, J.M.; Sieber, C.; Cooper, C.; Al-Daghri, N.; de Carvalho, I.A.; Bautmans, I.; Bernabei, R.; others. Assessment of muscle function and physical performance in daily clinical practice. *Calcified Tissue International* **2019**, pp. 1–14.
10. Spink, M.J.; Fotoohabadi, M.R.; Wee, E.; Hill, K.D.; Lord, S.R.; Menz, H.B. Foot and ankle strength, range of motion, posture, and deformity are associated with balance and functional ability in older adults. *Archives of physical medicine and rehabilitation* **2011**, *92*, 68–75.
11. McKean, M.R.; Burkett, B. The relationship between joint range of motion, muscular strength, and race time for sub-elite flat water kayakers. *Journal of Science and Medicine in Sport* **2010**, *13*, 537–542.
12. Barroso, F.; Bueno, D.R.; Gallego, J.Á.; Jaramillo, P.; Kilicarslan, A. Surface EMG in Neurorehabilitation and Ergonomics: State of the Art and Future Perspectives. In *Emerging Therapies in Neurorehabilitation*; Springer, 2014; pp. 267–284.
13. Martinez-Valdes, E.; Farina, D.; Negro, F.; Del Vecchio, A.; Falla, D. Early motor unit conduction velocity changes to high-intensity interval training versus continuous training. *Medicine & Science in Sports & Exercise* **2018**, *50*, 2339–2350.
14. Kang, H.G.; Dingwell, J.B. Dynamics and stability of muscle activations during walking in healthy young and older adults. *Journal of biomechanics* **2009**, *42*, 2231–2237.
15. Pfister, A.; West, A.M.; Bronner, S.; Noah, J.A. Comparative abilities of Microsoft Kinect and Vicon 3D motion capture for gait analysis. *Journal of medical engineering & technology* **2014**, *38*, 274–280.
16. Challis, J.H. The variability in running gait caused by force plate targeting. *Journal of Applied Biomechanics* **2001**, *17*, 77–83.
17. Cappozzo, A.; Della Croce, U.; Leardini, A.; Chiari, L. Human movement analysis using stereophotogrammetry: Part 1: theoretical background. *Gait & posture* **2005**, *21*, 186–196.
18. Heres, H.M.; Sjoerdsma, M.; Schoots, T.; Rutten, M.C.; van de Vosse, F.N.; Lopata, R.G. Image acquisition stability of fixated musculoskeletal sonography in an exercise setting: a quantitative analysis and comparison with freehand acquisition. *Journal of Medical Ultrasonics* **2020**, *47*, 47–56.
19. Nadzalan, A.M.; Mohamad, N.I.; Lee, J.L.F.; Chinnasee, C. Relationship between muscle architecture and badminton-specific physical abilities. *Human Movement* **2018**, *19*, 44–50.
20. Simpson, C.; Kim, B.; Bourcet, M.; Jones, G.; Jakobi, J. Stretch training induces unequal adaptation in muscle fascicles and thickness in medial and lateral gastrocnemii. *Scandinavian journal of medicine & science in sports* **2017**, *27*, 1597–1604.
21. Lento, P.H.; Primack, S. Advances and utility of diagnostic ultrasound in musculoskeletal medicine. *Current reviews in musculoskeletal medicine* **2008**, *1*, 24–31.
22. Pillen, S.; van Alfen, N. Skeletal muscle ultrasound. *Neurological research* **2011**, *33*, 1016–1024.
23. Kubo, K. Effects of static stretching on mechanical properties and collagen fiber orientation of the Achilles tendon in vivo. *Clinical Biomechanics* **2018**, *60*, 115–120.
24. Czyrny, Z. Standards for musculoskeletal ultrasound. *Journal of ultrasonography* **2017**, *17*, 182.
25. Giannakou, E.; Aggeloussis, N.; Arampatzis, A. Reproducibility of gastrocnemius medialis muscle architecture during treadmill running. *Journal of Electromyography and Kinesiology* **2011**, *21*, 1081–1086.
26. Chalchat, E.; Gennisson, J.L.; Peñailillo, L.; Oger, M.; Malgoyre, A.; Charlot, K.; Bourrilhon, C.; Siracusa, J.; Garcia-Vicencio, S. Changes in the Viscoelastic Properties of the Vastus Lateralis Muscle With Fatigue. *Frontiers in Physiology* **2020**, *11*, 307.
27. Sjoerdsma, M.; Fixsen, L.S.; Schoots, T.; van de Vosse, F.N.; Lopata, R.G. A demonstration of high field-of-view stability in hands-free echocardiography. *Cardiovascular Ultrasound* **2020**, *18*, 1–13.
28. Bouwmeester, S.; de Kleijn, M.; van Wijngaarden, J.; Houthuizen, P. The use of a probe stabilizer to reduce musculoskeletal overload of ultrasound operators in routine diagnostic echocardiographic imaging. *Journal of Ultrasonography* **2019**, *19*, 193.

29. Farup, J.; Kjølhede, T.; Sørensen, H.; Dalgas, U.; Møller, A.B.; Vestergaard, P.F.; Ringgaard, S.; Bojsen-Møller, J.; Vissing, K. Muscle morphological and strength adaptations to endurance vs. resistance training. *The Journal of Strength & Conditioning Research* **2012**, *26*, 398–407.
30. Murach, K.; Greever, C.; Luden, N.D. Skeletal muscle architectural adaptations to marathon run training. *Applied Physiology, Nutrition, and Metabolism* **2015**, *40*, 99–102.
31. Schoenfeld, B.J. The mechanisms of muscle hypertrophy and their application to resistance training. *The Journal of Strength & Conditioning Research* **2010**, *24*, 2857–2872.
32. Portilla, J.; Simoncelli, E.P. A parametric texture model based on joint statistics of complex wavelet coefficients. *International journal of computer vision* **2000**, *40*, 49–70.
33. Oppenheim, A.V.; Lim, J.S. The importance of phase in signals. *Proceedings of the IEEE* **1981**, *69*, 529–541.
34. Sampat, M.P.; Wang, Z.; Gupta, S.; Bovik, A.C.; Markey, M.K. Complex wavelet structural similarity: A new image similarity index. *IEEE transactions on image processing* **2009**, *18*, 2385–2401.
35. Xu, K.; Liu, X.; Cai, H.; Gao, Z. Full-reference image quality assessment-based b-mode ultrasound image similarity measure. *arXiv preprint arXiv:1701.02797* **2017**.
36. Otsu, N. A threshold selection method from gray-level histograms. *IEEE transactions on systems, man, and cybernetics* **1979**, *9*, 62–66.
37. Cunningham, R.J.; Harding, P.J.; Loram, I.D. The application of deep convolutional neural networks to ultrasound for modelling of dynamic states within human skeletal muscle. *arXiv preprint arXiv:1706.09450* **2017**.
38. Kumar, A.; Anel, R.; Bunnell, E.; Habet, K.; Zanotti, S.; Marshall, S.; Neumann, A.; Ali, A.; Cheang, M.; Kavinsky, C.; others. Pulmonary artery occlusion pressure and central venous pressure fail to predict ventricular filling volume, cardiac performance, or the response to volume infusion in normal subjects. *Critical care medicine* **2004**, *32*, 691–699.
39. Simonsen, J.G.; Axmon, A.; Nordander, C.; Arvidsson, I. Neck and upper extremity pain in sonographers–associations with occupational factors. *Applied ergonomics* **2017**, *58*, 245–253.
40. Evans, K.; Roll, S.; Baker, J. Work-related musculoskeletal disorders (WRMSD) among registered diagnostic medical sonographers and vascular technologists: a representative sample. *Journal of Diagnostic Medical Sonography* **2009**, *25*, 287–299.
41. Hodges, P.; Pengel, L.; Herbert, R.; Gandevia, S. Measurement of muscle contraction with ultrasound imaging. *Muscle & Nerve: Official Journal of the American Association of Electrodiagnostic Medicine* **2003**, *27*, 682–692.
42. Kellis, E.; Galanis, N.; Natsis, K.; Kapetanos, G. Validity of architectural properties of the hamstring muscles: correlation of ultrasound findings with cadaveric dissection. *Journal of biomechanics* **2009**, *42*, 2549–2554.